Front. Optoelectron. China 2011, 4(2): 166–170
DOI 10.1007/s12200-011-0157-6

RESEARCH ARTICLE

Silver nanoparticles and silver molybdate nanowires complex for surface-enhanced Raman scattering substrate

Zhiyong BAO[1], Li ZHANG (✉)[2], Yucheng WU (✉)[1]

1 College of Material Science and Engineering, Hefei University of Technology, Hefei 230009, China
2 Anhui Key Laboratory of Spin Electron and Nanomaterials (Cultivating Base), Department of Chemistry and Life Science, Soochow University, Suzhou 234000, China

Abstract Selective synthesis of silver and uniform single crystalline silver molybdate nanowires in large scale can be easily realized by a facile soft template approach. $Ag_6Mo_{10}O_{33}$ nanowires with a uniform diameter of about 50 nm and the length up to several hundred micrometers were synthesized in large scale for the first time at room temperature using 12-silicotungstic acid system. The silver nanoparticles can be easily synthesized with the assistance of UV-light. Sensitive surface-enhanced Raman scattering signals of p-aminothiophenol were observed on Ag nanoparticles and silver molybdate nanowires complex. The results demonstrated that synthetic method could be a potential mild way to selectively synthesize various molybdate nanowires with various phases in large scale. The silver nanoparticles and silver molybdate nanowires complex would be proposed for surface-enhanced Raman scattering substrate.

Keywords 12-tungstosilicate acid, hydrothermal approach, surface-enhanced Raman scattering

1 Introduction

Molybdenum is a kind of important inorganic materials and can be widely used in the photoluminescence [1], microwave [2], fiber optic [3], scintillator [4], humidity sensors [5], magnetic [6], catalyst [7], and other aspects [8]. The previously reported synthetic methods of molybdate, mostly had been performed at high temperature or required other harsh conditions, such as at 1000°C under solid state metal exchange reaction [9], or sol-gel process [10]. There have been few reports on the synthesis of this kind of materials by hydrothermal/solvothermal methods [11]. The molybdate (such as $Ag_2Mo_4O_{13}$, $Ag_2Mo_2O_7$ and Ag_2MoO_4) is made by MoO_3 and Ag_2O mixed by a certain proportion and then sintered with high temperature [12]. These materials have high electrical conductivity, which have been normally applied in conductive glass [13]. Yu's group reported the synthesis of single-crystal silver molybdate/tungstate nanowires with hydrothermal process, showing a selective synthesis of uniform single crystalline silver molybdate/tungstate nanorods/nanowires in large scale by a facile hydrothermalre crystallization technique [14]. Shao et al. have observed the ultrasensitive surface-enhanced Raman scattering (SERS) signals of four typical analytes on Ag nanoparticles (NPs) from β-silver vanadate and copper, even though the concentrations of these analytes were very low [15].

In this paper, we reported on how to synthesize silver molybdate nanowires in the liquid phase at room temperature using 12-silicotungstic acid system. Then, the above mixture solution was irradiated with ultraviolet (UV) light. Finally, the silver nanoparticles coving on the surface of silver molybdate nanowires (SMNs) can be synthesized. The experimental device in this method is simple, easy to operate and applicable to a large scale synthesis. This new and universal method for preparing a substrate for the detection of surface-enhanced Raman spectroscopy is proposed.

2 Experiments

2.1 Materials

Tungstosilicate acid [$H_4(SiW_{12}O_{40})$, TSA], silver nitrate ($AgNO_3$), Na_2MoO_4 and ethanol were all of A.R. grade and obtained from Shanghai Reagent Co. and were used without further purification. p-aminothiophenol (PATP)

Received November 1, 2010; accepted November 30, 2010

E-mail: zhlisuzh@163.com, ycwu@hfut.edu.cn

was purchased from Sigma-Aldrich and used without further purification. Doubly distilled water was used throughout experiments to prepare the solutions.

2.2 Characterizations

The X-ray diffraction (XRD) analysis was carried out with a MAP18AHF instrument (Japan MAC Science Co.). The morphologies and structures of the nanoparticles were examined by FEI Sirion-200 field emission scanning electron microscope (SEM) and JEOL 2010 transmission electron microscope (TEM). The macro-SERS spectra were recorded with a Renishaw Raman RM2000 equipped with the 514.5 nm laser line, an electrically refrigerated CCD camera, and a notch filter to eliminate the elastic scattering. The spectra shown here were obtained with a 30 mm focus length lens. The output of laser power on the sample was about 2 mW. The spectral resolution was 4 cm^{-1}. The spectral scanning conditions were chosen to avoid sample degradation. The reported spectra were registered as single scans. Pyris-I TGA Analyzer (Perkin-Elmer Corporation), the temperature of the sample rose at constant speed (10°C/min) in N_2 atmosphere during heating.

2.3 Preparation of silver and silver molybdate complex

In a typical experiment, 2-propanol (2 mL) and deaerated solution of tungstosilicate acid (30 mL, 2 mM) were added to an aqueous deaerated solution of $AgNO_3$ (15 mL, 4 mM solution), and then the solution of Na_2MoO_4 (15 mL, 4 mM) was added to the above mixture with continuous stirring for 30 min and then was allowed to age for 2 h. A homogeneous light-yellow solution at room temperature was formed, indicating the formation of silver molybdate. When the above mixture was irradiated with UV light (Pyrex filter, > 280 nm, 450 W Hanovia medium pressure lamp) for 2 h at the same time, the solution turned gray gradually, indicating the formation of the silver and silver molybdate complex. The yields were collected and washed several times using the double distilled water, dried in a vacuum oven at the 60°C for 6 h. The Ag NPs concentration was measured by UV-visible spectroscopy using the molar extinction coefficients at the wavelength of the maximum absorption of Ag colloid.

3 Results and discussion

XRD pattern shown in curve 1 of Fig. 1 was recorded from a drop coated film of the non UV-irradiated sample on a glass substrate. All reflection peaks of the products can be indexed as a pure structure with cell parameters $a = 7.59$ Å, $b = 8.31$ Å, $c = 11.42$ Å, which is in good agreement with the literature value (JCPDS Card: 72–1689). Pure

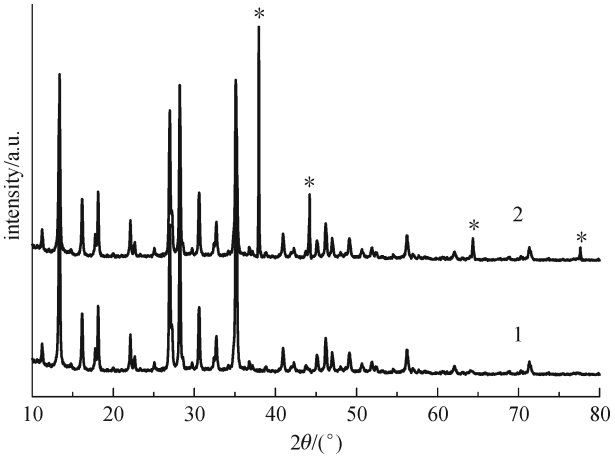

Fig. 1 XRD patterns recorded from drop-coated films on glass substrates of silver molybdate synthesized by reaction of TSA solution with aqueous $AgNO_3$ and Na_2MoO_4, before (curve 1) and after (curve 2) UV irradiation (Bragg reflections marked * correspond to Ag)

$Ag_6Mo_{10}O_{33}$ phase can be obtained in TSA system at pH 2 [16]. Curve 2 of Fig. 1 shows the XRD pattern of the UV-irradiated sample. The (111), (200), (220), and (311) Bragg reflections of face-centered cubic (fcc) silver are clearly observed (indicated by an asterisk). Some of the Bragg reflections corresponding to the $Ag_6Mo_{10}O_{33}$ phase structure indicate that the formation of silver nanoparticles on the $Ag_6Mo_{10}O_{33}$ colloidal particle template does not disrupt the basic structure of silver molybdates.

In this study, a solution method was employed to synthesize SMNs. The SEM image (Fig. 2(a)) reveals that the SMNs are generally ultralong with the length up to several hundred micrometers. When the reaction solution was irradiated by UV-light simultaneously, fresh silver nanoparticles were produced *in situ*. Figure 2(b) displays an SEM image of the SMNs covered with Ag nanoparticles. TEM image in Fig. 2(c) shows that the particles are also rod-like and the diameter is about 50 nm. The surface structures indicate that the crystal surface is smooth. The inset of Fig. 2(c) shows the associated selected-area electron diffraction (SAED) pattern recorded by focusing the incident electron beam on an individual nanowire, and exhibits the single-crystalline nature of the wire. We have also carried out extensive investigations on more individual wires by using electron diffraction (ED), and the results demonstrate that the as-synthesized sample is single-crystalline. Based on the XRD pattern and the electron diffraction pattern, we concluded that the nanowires grow preferentially along *c* axis. The TEM image (Fig. 2(d)) shows that the SMNs were almost completely covered with Ag nanoparticles with an average diameter of 16 nm. The high resolution TEM images in Fig. 2(e) show that very tiny nanoparticles sized from 10 to 25 nm are attached on the backbone of the SMNs.

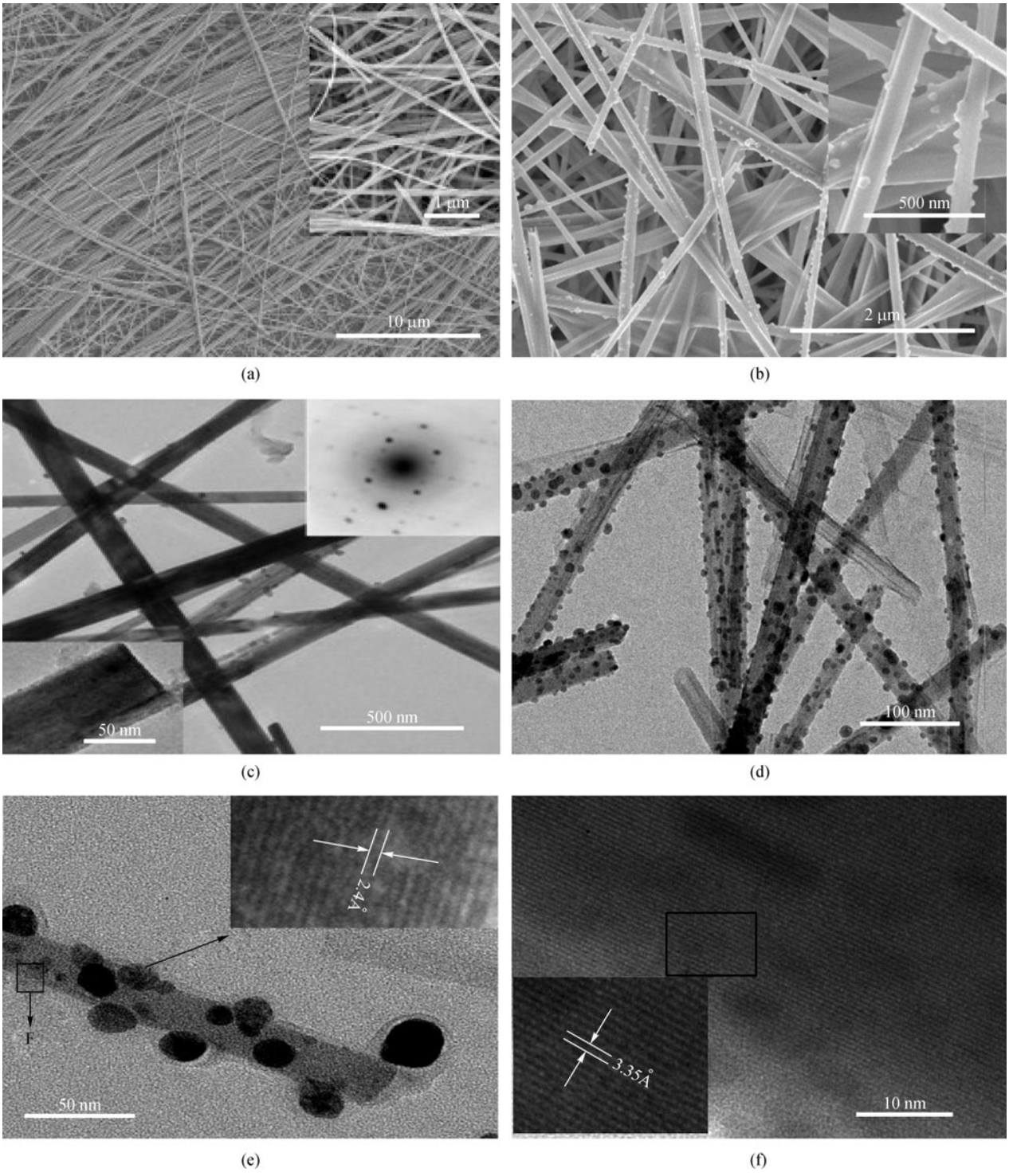

Fig. 2 A solution method was employed to synthesize SMNs. (a) SEM images of SMNs; (b) SEM images of SMNs covered with Ag nanoparticles; (c) TEM images of SMNs; insets of (c) are individual SMN and electron diffraction pattern; (d) TEM images of SMNs covered with Ag nanoparticles; (e) TEM image of individual SMN covered with Ag nanoparticles, inset shows crystal-lattice image of an individual Ag nanoparticle and SMN; (f) crystal-lattice image of individual SMN

Interestingly, the silver nanoparticles were not observed to be separated from the SMNs in the solution, which indicates that the Ag^+ reduction occurrs on the surface of the $Ag_6Mo_{10}O_{33}$ colloidal particles and suggests that the $Ag_6Mo_{10}O_{33}$ colloidal particles act as excellent templates. From the insets of Figs. 2(e) and 2(f), Ag NPs and SMN were single crystals, and they grow along the [111] and [022] axis. The crystal lattices of Ag and $Ag_6Mo_{10}O_{33}$ may be indexed as (111) and (022) crystal planes with 0.24 and 0.335 nm corresponding to Ag (111) plane and $Ag_6Mo_{10}O_{33}$ (022) plane, respectively.

It is interesting that more and more other tiny nanoparticles have appeared on the backbone of the $Ag_6Mo_{10}O_{33}$ nanowire after its exposure under electron beam irradiation. Clearly, this nanoline is unstable with electron beam irradiation. Nanoparticles on the surface get increased gradually as the time for the electron beam irradiation is prolonged. Accordingly, it is deduced that the melting point of this compound is likely low. Figure 3 shows the results of $Ag_6Mo_{10}O_{33}$ nanowires differential thermal analysis. It reveals that the compound melting point is about 236°C, which is not high. This can explain the phenomenon under electron beam irradiation. Large heat is generated because of electron beam bombardment. Nanoline partially melts and amorphous particles are formed after its structure is destroying. At the same time, electron diffraction results — whose data is not presented — show that these new nanoparticles in the experimental process is amorphous. These results are consistent with the phenomenon observed by Yu [14].

Herein, a unique approach to prepare a SERS substrate is proposed by utilizing silver molybdate as raw materials. Silver molybdate nanowires in large scale are synthesized through a simple solution approach at room temperature. Then, silver nanoparticles are obtained using UV light to irradiate silver molybdate solution, and Ag nanoparticles are covered on the surface of the silver molybdate *in situ*. Solution synthesis of the silver and silver molybdates nanowires complex is not found in literature up to now. The Ag-SMNs complex demonstrated the sensitivity in the SERS detection of PATP, which is similar to the SERS substrate of Ag nanoparticles covered on β-silver vanadate nanowires [14].

On the basis of theoretical calculations combined with the reports in literatures, Wu et al. [17] demonstrated that the PATP molecules adsorbed on nanoscale rough surfaces of noble metals and nanoparticles undergo a catalytic coupling reaction to selectively produce a new surface species p,p′-dimercaptoazobenzene (DMAB). There are no fundamentals found in their cluster model calculations, which matches the vibrational frequencies of 1142, 1391, and 1440 cm^{-1} as observed in SERS of PATP on rough electrodes and nanoparticles of silver [18–20]. The peak positions of these intense SERS bands observed in experiments cannot be reproduced in their calculations of PATP interacting with various silver clusters. They [17] concluded that the experimentally observed bands do not arise directly from PATP adsorbed on silver surfaces. Therefore, the phenomenon in SERS of PATP should be with some new surface species, DMAB. In our study, we observed the same experiment phenomenon. Figure 4 is the SERS spectra from PATP modified Ag-SMNs complex compared with the Raman spectra of the solid PATP. The Raman spectrum of the solid PATP (curve 1) is different from that of PATP modified Ag-SMNs under the light irradiation (curve 2). The peaks at 1139, 1389, or 1432 cm^{-1} as observed in our SERS spectra (curve 2) can be attributed to that the DMAB is produced from the catalytic coupling reaction of PATP on rough silver nanoparticles surfaces under the nanoparticle-assisted photonic catalytic oxidation, which is different from the results of the electrochemical process [21].

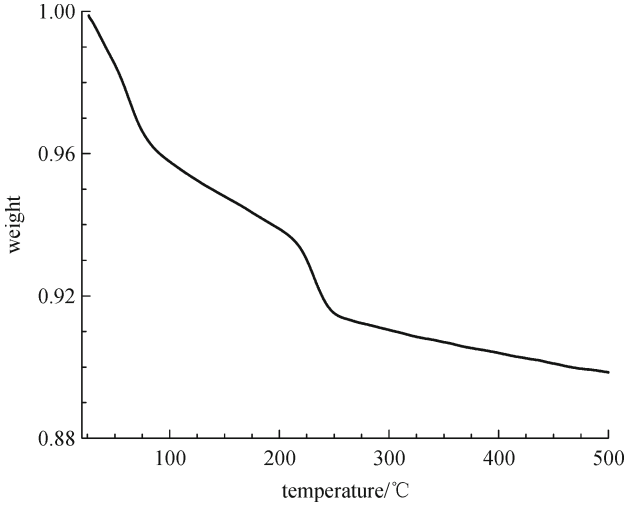

Fig. 3 Differential thermal analysis of $Ag_6Mo_{10}O_{33}$ nanowires

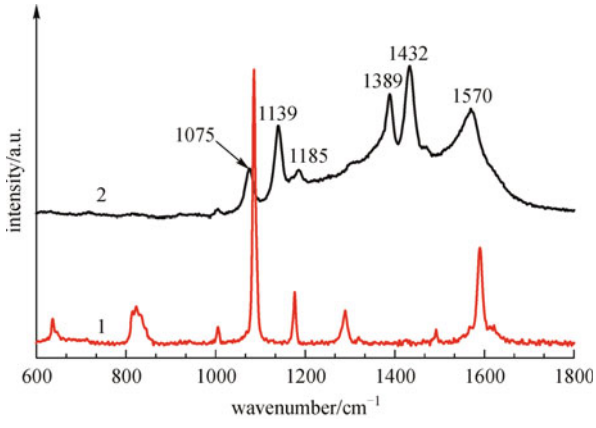

Fig. 4 Raman and SERS spectra of solid PATP (curve 1), and SERS (curve 2) spectra from PATP modified Ag-SMNs complex

4 Conclusion

In summary, silver and silver molybdate nanowires complex can be synthesized in the 12-silicotungstic acid system. Ag-Silver molybdate nanowires complex are demonstrated to be a new style SERS substrate.

Acknowledgements This work was supported by the National Natural Science Foundation of China (NSFC) (Grant No. 20871089), and the Important Projects of Anhui Provincial Education Department (No. KJ2010ZD09).

References

1. Qi T, Takagi K, Fukazawa J. Scintillation study of $ZnWO_4$ single crystals. Applied Physics Letters, 1980, 36(4): 278–279
2. van Uitert L G, Preziosi S. Zinc tungstates for microwave maser applications. Journal of Applied Physics, 1962, 33(9): 2908–2909
3. Rushbrcoke J G, Ansorge R E. Optical fibre readout and performance of small scintillating crystals for a fine-grained gamma detector. Nuclear Instruments and Methods in Physics Research Section A, 1989, 280(1): 83–90
4. Tanaka K, Miyajima T, Shirai N, Zhuang Q, Nakata R. Laser photochemical ablation of $CdWO_4$ studied with the time-of-flight mass spectrometric technique. Journal of Applied Physics, 1995, 77 (12): 6581–6587
5. Qu W, Wlodarski W, Meyer J U. Comparative study on micromorphology and humidity sensitive properties of thin-film and thick-film humidity sensors based on semiconducting $MnWO_4$. Sensors and Actuators B, 2000, 64(1–3): 76–82
6. Ehrenberg H, Weitzel H, Held C, Fuess H, Wltschek G, Kroener T, van Tol J, Bonnet M. Magnetic phase diagrams of $MnWO_4$. Journal of Physics: Condensed Matter, 1997, 9(15): 3189–3203
7. Sleight A W. Structural crystallography and crystal chemistry. Acta Crystallographica Section B, 1972, 28(10): 2899–2902
8. Chamberland B L, Kafalas J A, Goodenough J B. J. A. KaMlas, J. B. Goodenough. Characterization of chromium manganese oxide ($MnCrO_3$) and chromium (III) manganate. Inorganic Chemistry, 1977, 16(1): 44–46
9. Swanson H E, Morris M C, Stanchfield R P, Evans E H. 3D architectures of iron molybdate: phase selective synthesis. National Bureau of Standards Monograph, 1963, 25: 24–35
10. Bonanni M, Spanhel L, Lerch M, Füglein E, Müller G, Jermann F. Conversion of colloidal ZnO-WO_3 heteroaggregates into strongly blue luminescing $ZnWO_4$ xerogels and films. Chemistry of Materials, 1998, 10(1): 304–310
11. Li Y B, Bando Y, Golberg D, Uemura Y. SiO_2-sheathed InS nanowires and SiO_2 nanotubes. Applied Physics Letters, 2003, 83 (19): 3999–4001
12. Obare S O, Jana N R, Murphy C J. Preparation of polystyrene-and silica-coated gold nanorods and their use as templates for the synthesis of hollow nanotubes. Nano Letters, 2001, 1(11): 601–603
13. Yin Y D, Lu Y, Sun Y G, Xia Y N. Silver nanowires can be directly coated with amorphous silica to generate well-controlled coaxial nanocables of silver/silica. Nano Letters, 2002, 2(4): 427–430
14. Cui X J, Yu S H, Li L L, Biao L, Li H B, Mo M S, Liu X M. Selective synthesis and characterization of single-crystal silver molybdate/tungstate nanowires by a hydrothermal process. Chemistry, 2004, 10(1): 218–223
15. Shao M W, Lu L, Wang H, Wang S, Zhang M L, Ma D D D , Lee S T. An ultrasensitive method: surface-enhanced Raman scattering of Ag nanoparticles from β-silver vanadate and copper. Chemical Communications, 2008, (20): 2310–2312
16. Cañamares M V, Garcia-Ramos J V, Gómez-Varga J D, Domingo C, Sanchez-Cortes S. Ag nanoparticles prepared by laser photoreduction as substrates for *in situ* surface-enhanced Raman scattering analysis of dyes. Langmuir, 2007, 23(9): 5210–5215
17. Wu D Y, Liu X M, Huang Y F, Ren B, Xu X, Tian Z Q. Surface catalytic coupling reaction of p-mercaptoaniline linking to silver nanostructures responsible for abnormal SERS enhancement: a DFT study. Journal of Physical Chemistry C, 2009, 113(42): 18212–18222
18. Hill W, Wehling B. Potential- and PH-dependent surface-enhanced Raman scattering of p-mercapto aniline on silver and gold substrates. Journal of Physical Chemistry, 1993, 97(37): 9451–9455
19. Osawa M, Matsuda N, Yoshii K, Uchida I. Charge transfer resonance Raman process in surface-enhanced Raman scattering from p-aminothiophenol adsorbed on silver: Herzberg-Teller contribution. Journal of Physical Chemistry, 1994, 98(48): 12702–12707
20. Zhou Q, Li X W, Fan Q, Zhang X X, Zheng J W. Charge transfer between metal nanoparticles interconnected with a functionalized molecule probed by surface-enhanced Raman spectroscopy. Angewandte Chemie International Edition, 2006, 45(24): 3970–3973
21. Riskin M, Tel-Vered R, Lioubashevski O, Willner I. Ultrasensitive surface plasmon resonance detection of Trinitrotoluene by a bisaniline-cross-linked Au nanoparticles composite. Journal of American Chemical Society, 2009, 131(21): 7368–7378